Chapter 12
Production of the Atmospheric Oxidant Radicals OH and HO_2 from the Ozonolysis of Alkenes

William J. Bloss, M.S. Alam, A.R. Rickard, M. Camredon, K.P. Wyche, T. Carr, and P.S. Monks

Abstract The reactions of ozone with alkenes are of importance within atmospheric chemistry as a non-photolytic source of the oxidant radicals OH, HO_2 and RO_2. While OH yields are relatively well constrained, few data exist for production of HO_2 or RO_2. We report direct measurements of total radical yields from a range of small (C_2–C_5) alkenes, using LIF and PERCA techniques within large simulation chamber experiments. OH yields are found to be consistent with established understanding, while HO_2 yields are substantially smaller than previous measurements suggest, but in good agreement with those assumed within current atmospheric chemical mechanisms.

Keywords Troposphere • Alkenes • Ozonolysis • OH • HO_2

12.1 Introduction

Alkenes, unsaturated hydrocarbons, are emitted to the atmosphere from a range of natural and anthropogenic sources, notably biogenic emissions of isoprene, C_5H_8, and the isoprenoid terpenes (C_{10}) and sesquiterpenes (C_{15}). Alkenes can contribute up to 30% of the total OH sink in urban regions, and a higher proportion forested environments; atmospheric degradation of alkenes contributes to the production of ozone in the presence of nitrogen oxides, and leads to the production of substituted and/or oxygenated degradation products, which may act as precursors to, or contribute to the formation of, secondary organic aerosol (SOA). In addition to degradation driven by reaction with OH and NO_3, alkene oxidation may be initiated by reaction with ozone, a process which leads to the dark, non-photolytic production of

W.J. Bloss (✉) • M.S. Alam • A.R. Rickard • M. Camredon • K.P. Wyche • T. Carr • P.S. Monks
School of Geography, Earth & Environmental Sciences, University of Birmingham, Birmingham B15 2TT, UK
e-mail: w.j.bloss@bham.ac.uk

I. Barnes and K.J. Rudziński (eds.), *Disposal of Dangerous Chemicals in Urban Areas and Mega Cities*, NATO Science for Peace and Security Series C: Environmental Security,
DOI 10.1007/978-94-007-5034-0_12,

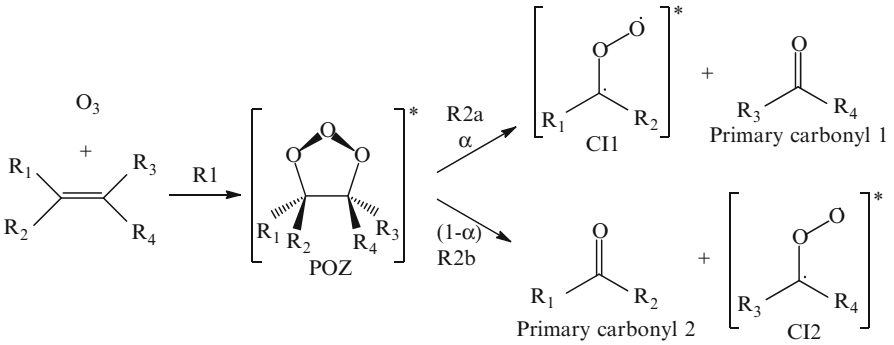

Fig. 12.1 Cycloaddition of ozone across the alkene double bond and subsequent decomposition of the POZ – The "Criegee Mechanism"

radical intermediates; detailed analyses of measurements from atmospheric field campaigns have shown ozonolysis to account for up to 30% of the total OH radical production. Understanding the yields of OH, HO_2 and RO_2 radicals, and their dependence upon atmospheric conditions, is essential to quantify this important contribution to atmospheric oxidising capacity.

Gas-phase alkene ozonolysis is believed to proceed *via* the Criegee mechanism [7], illustrated in Fig. 12.1. Ozonolysis is highly exothermic, initiated by the electrophilic cycloaddition of ozone across the C=C double bond to form an unstable 1,2,3-trioxolane (hereafter referred to as a primary ozonide, POZ) (R1). This intermediate is high in energy and rapidly decomposes at the central C–C bond and one of the O–O bonds. Given that the O–O bond can break at two different sites, a pair of carbonyl oxides (hereafter referred to as Criegee Intermediates, CIs) and stable carbonyl molecules can be formed (R2a and R2b).

The CI and carbonyl co-product produced from the exothermic decomposition of the POZ possess a significant amount of vibrational excitation. This energy enables further unimolecular reactions of the excited CI to occur but is not sufficient for the decomposition of the carbonyl molecule [6] – Fig. 12.2. The distribution of decomposition products of the POZ is dependent upon the substitution of the alkene. Different CIs behave as distinct chemical entities as demonstrated by the range of detected experimental products, dependent upon the extent of the substitution of the CI and distribution of energy following decomposition of the POZ. Substituted CIs can be formed in a *syn* (*i.e.* with the alkyl substituent on the same side of the CI as the terminal O atom) configuration or *anti* configuration, with a substantial barrier to interconversion between them. Briefly, *syn*- and di-substituted CIs are thought to predominantly decompose through isomerisation via a five-membered transition state to give an excited hydroperoxide species which subsequently decomposes to give OH and a vinoxy radical (the "hydroperoxide mechanism" – e.g. [17] and references therein). The proportion of the vibrationally excited CI that does not isomerise/decompose is suggested to be collisionally stabilised and can therefore undergo bimolecular reactions [25]. In general, at low pressures, energy rich

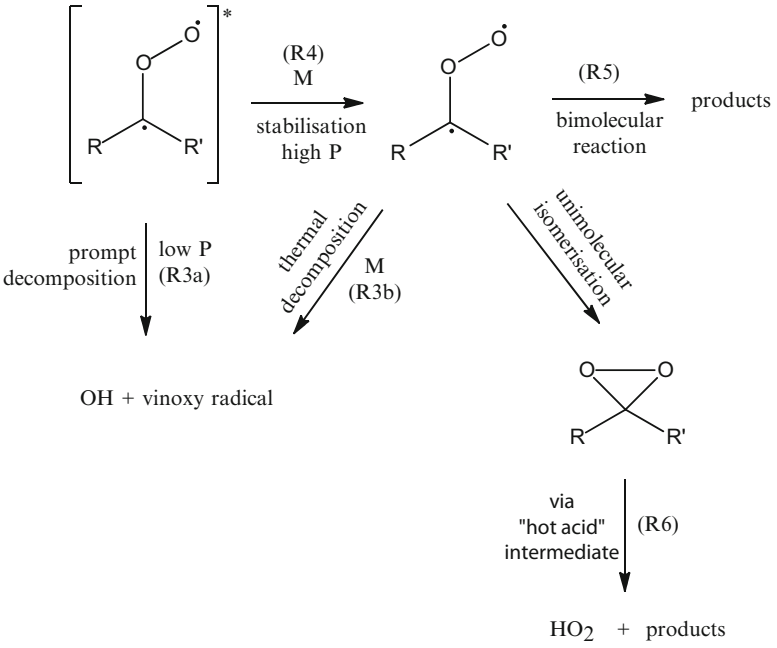

Fig. 12.2 Potential fates of the Criegee intermediate

CIs undergo prompt decomposition to yield OH and a vinoxy radical, which subsequently reacts near-instantaneously with O_2 to form a peroxy radical [9]. At higher pressures (*i.e.* under boundary layer conditions) the CI may be collisionally stabilised (Fig. 12.2, R4) and can thermally decompose to generate OH and a vinoxy radical (R3b) or undergo rearrangement through a dioxirane structure. The dioxirane structure can decompose to various products including HO_2 (R6), *via* a 'hot' acid intermediate.

The vinoxy radical formed alongside OH (Fig. 12.2) will react with oxygen in the atmosphere to form an excited β-oxo peroxy radical, which may be stabilised or undergo decomposition forming CO, a (secondary) stable carbonyl species and OH [19]. However, this pathway to OH formation is only thought to be significant if an aldehydic hydrogen is present. The stabilised β-oxo peroxy radical may then undergo self- or cross-reaction with other peroxy radicals to form stable species such as glyoxal, glycolaldehyde, peroxides and secondary carbonyls.

The fate of the *anti*-CI and of the CH_2OO CI formed from terminal alkenes is discussed in detail elsewhere [1]. Briefly, the *anti*-CI (and CH_2OO) can undergo rearrangement through a dioxirane structure, which can decompose to various products including OH, HO_2, CO, CO_2, H_2O and alkyl molecules *via* a 'hot' acid/ester intermediate (*e.g.* [6]). The *syn* and *anti*-CIs can also undergo stabilisation followed by bimolecular reaction, but studies suggest that stabilisation is a minor process for di-substituted and *syn* mono-substituted CIs, as their lifetime with respect to the vinyl hydroperoxide mechanism is thought to be substantially shorter than the time required for bimolecular processes to occur [10, 26]. Collisional

stabilisation is therefore more likely to occur for the *anti*-CI (for which the hydroperoxide route is unavailable), potentially enabling bimolecular reactions to proceed with many atmospherically relevant species such as H_2O, NO_2, SO_2 and CO [6, 13, 18]. In this article we review the results of a detailed study of the ozonolysis of a series of small-chain alkenes (ethene – isoprene), with a focus upon the production of the radical species OH an HO_2, and their dependence upon experimental conditions (e.g. humidity).

12.2 Experimental Approach

The experimental work was performed in the European Photoreactor (EUPHORE) in Valencia, Spain, coupled with detailed chemical box modelling analysis for data interpretation. The EUPHORE facility comprises two large scale atmospheric simulation chambers, used for studying the mechanisms of atmospheric processes. Briefly, each chamber consists of a 197 m^3 hemispherical reactor, formed from fluorine-ethene-propene (FEP) Teflon foil (127 μm thickness), and fitted with housings which exclude ambient sunlight. Detailed descriptions of the chambers and their instrumentation are given elsewhere [3]. In this study a range of analytical instrumentation was used, including traditional monitors (O_3, CO, HCHO, H_2O), Fourier transform infrared spectroscopy (FTIR) and chemical ionisation reaction time-of-flight mass-spectrometry (CIR-TOF-MS – [34]) for the detection of precursor and product species, including oxygenated derivatives. Radical species were monitored using laser induced fluorescence (LIF – [4, 32]) and peroxy radical chemical amplifier (PERCA – [12]) for the detection of OH/HO_2 and $HO_2 + \Sigma RO_2$ respectively.

All ozonolysis experiments were performed with the chamber housings closed to exclude ambient light/photochemical effects ($j(NO_2) < 2 \times 10^{-6}$ s^{-1}), at near atmospheric pressure and at ambient temperature (294–298 K). All experiments were conducted under NO_x-free conditions. In the absence of NO_x and sunlight, chamber wall radical production has been shown to be negligible [35]. For "dry" experiments, the relative humidity was low (in simulation chamber terms: <1% RH). The experimental procedure, starting with a clean flushed chamber (NMHC < 0.2 ppbV, CH_4 = ambient *i.e.* 1,800 ppbV, NO_y < 1 ppbV), was to add SF_6 (as a dilution tracer), followed by ozone (50–500 ppbV) and in certain cases an OH scavenger (CO or cyclohexane, in concentrations such that ≥95% of any OH produced was scavenged rather than reacting with the precursor alkene) was introduced prior to ozone injection. To initiate the reaction, a known aliquot of alkene (20–500 ppbV) was injected into the chamber and the evolution of reactants and products monitored over timescales of 1–3 h, at a time resolution ranging from seconds (e.g. LIF) to 10 min (FTIR scan time). For "wet" experiments, where the relative humidity was increased to *ca.* 30%, water was added to the chamber through a nebuliser prior to the addition of the reactants.

The EUPHORE data was analysed using a detailed chemical box model, based upon the Master Chemical Mechanism (MCM: http://mcm.leed.ac.uk/MCM) version 3.1 [5, 15, 31], incorporating an extended and updated version of the ozonolysis mechanism of interest (*c.f.* [1]). Within the model, the POZ and CI were assumed to decompose rapidly (compared with the timescale of the subsequent chemistry) to form radical products and stable species, or stabilised CIs, and were therefore not assigned individual rate constants. Rate constants for the bimolecular reactions of the SCI were taken directly from the MCM. The cyclohexane photo-oxidation mechanism, extracted from MCMv3.1, was also updated and extended as outlined in Alam et al. [1]. Simulations were initialised at the time point at which the maximum measured alkene mixing ratio was observed. Temperature, relative humidity and dilution rates were averaged over the duration of each experiment, as the variation in these parameters on the experimental timescale was minimal. Four analytical stages were performed, in each case to determine the *overall* yields of specific products from the *overall* fast ozonolysis reaction (i.e. the CI formation/decomposition chemistry). Briefly, alkene/O_3 reaction rate coefficients were optimised for experiments performed in the presence of a radical scavenger, followed by the optimisation of the branching ratios of the POZ decomposition, forming the respective pairs of carbonyl products (and CIs). Overall carbonyl yields were derived using model optimisation, by minimising the sum of squares of residuals between the simulated and observed concentrations, and classically, by (dilution corrected) mass balance calculations; both methods were in excellent agreement. Finally, HO_x radical yields were determined by optimising the branching ratio for the isomerisation/decomposition of the *syn*-CI to minimise the sum of squares of residuals between simulated and observed OH/HO_2 concentrations. The OH yield from the ozonolysis of ethene (0.17; [1]) was applied to the decomposition of the CH_2OO CI formed in all terminal alkene systems. The model optimization process accounted for further reactions of OH and HO_2, and for secondary formation processes. It is important to note that the overall HO_x yields obtained through this approach, relative to flux through each alkene-ozone reaction, are reasonably absolute and independent of the HO_x production route implemented in the model, but their attribution to specific reaction pathways of the ozonolysis system (*e.g.* Criegee decomposition branching ratios) is dependent upon the assumed mechanism. In the discussion below we draw inferences regarding the likely mechanistic origin of the observed OH and HO_2, from the variation in yields with co-products and experimental conditions.

12.3 OH Production

Figure 12.3 shows a typical temporal profile of the OH steady state concentration as measured by the LIF system, and model simulation comparisons for cis-2-butene ozonolysis. The data illustrate that MCMv3.1 overestimates (in the case of cis-

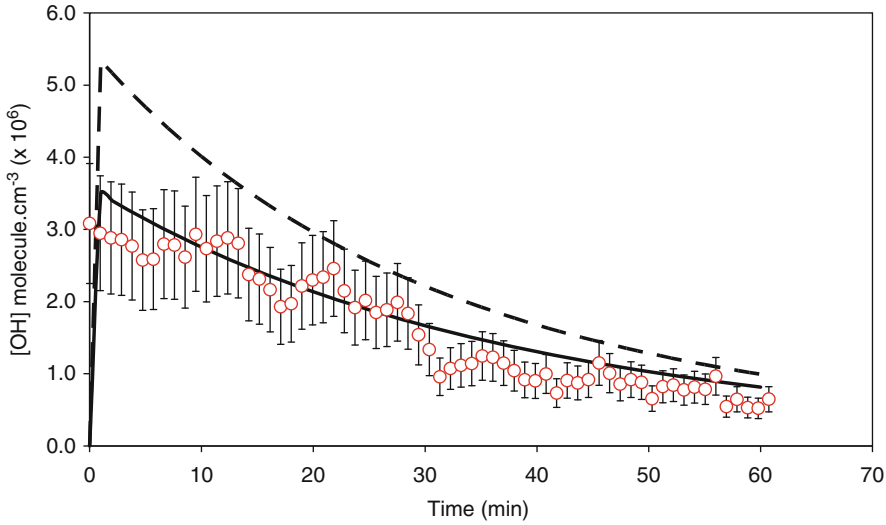

Fig. 12.3 *cis*-2-Butene ozonolysis. Temporal profile of OH (*circles*) plus model simulations before (*dashed line*, base case standard MCMv3.1 chemistry) and after (*solid line*) optimising the OH yield

2-butene) the OH yield, compared to the present work. (In this instance it is likely that this arises from the assumed 50:50 split of the *syn*/*anti* CIs in the MCM 3.1 mechanism – the lower yield obtained here (and in other studies – [14]) suggests that the *anti*-conformer of the CI is preferentially formed (alongside acetaldehyde) from the primary ozonide decomposition in this system – [29]).

Figure 12.4 shows the OH yields obtained for ethene, propene, 1-butene, 2-methylpropene, cis-2-butene, trans-2-butene and 2,3-dimethyl-2-butene, compared to those from other studies [2, 23, 24, 27, 28, 30] plotted as a function of the equivalent IUPAC recommendations for OH yields [14]. The uncertainties in the results from this work represent the combined (2σ) statistical uncertainty from repeated determinations propagated with the corresponding OH measurement calibration uncertainty (27%; [4]). The results are well correlated with the IUPAC values; as the literature studies mainly exploit indirect methods to detect OH, by the use of OH scavenger (*e.g.* [2]) and tracer (*e.g.* [30]) techniques, or indirect observation by matrix-isolation electron spin resonance [24] and PERCA [28] the agreement with the direct OH observations in this work is encouraging. The results are consistent with the isomerisation/decomposition of a given CI to a vinyl hydroperoxide and OH; the basis of the OH yield structure activity relationship (SAR) of Rickard et al. [30].

These OH production *yields* (Y_{OH}) correspond to the formation of OH via the (fast) direct decomposition/isomerisation of the CI, after taking secondary sources into account within the model; for example OH formation via $HO_2 + O_3$, from decomposition of the excited β-oxo peroxy radical [19] and the reactions of acyl peroxy radicals + HO_2 [8, 16].

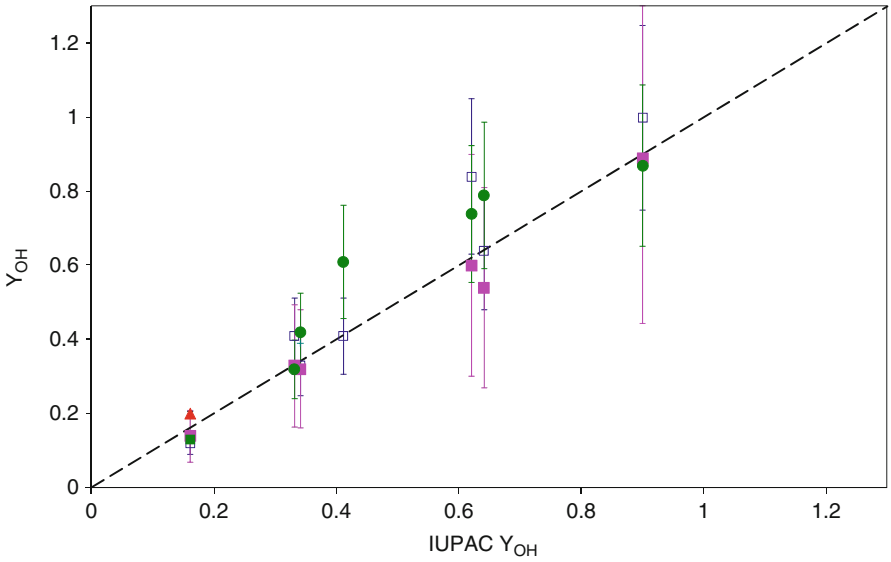

Fig. 12.4 Comparison of the OH yields from this work and literature studies, with the current [14] OH yield recommendations (abscissa). *Filled circles*: this work; *filled squares*: Rickard et al. [30]; *open squares*: Atkinson et al. [2]; *filled triangle*: Mihelcic et al. [24]. The *dashed line* shows the 1:1 correlation

12.4 HO_2 Production

The yields of HO_2 (Y_{HO2}) for the alkenes studied were found to be significantly larger in the absence of OH radical scavengers (specifically, carbon monoxide) – particularly for the 2-methylpropene and 2,3-dimethyl-2-butene ozonolysis systems, where "Y_{HO2}" values were found to be significantly greater than unity (1.51 and 1.74 respectively). It is likely that in the absence of radical scavengers the retrieved HO_2 concentrations are in fact biased high due to interference from the decomposition of β-hydroxyalkyl peroxy radicals, formed from the OH + alkene reactions, within the LIF instrument [11]. We therefore disregard the HO_2 observations/yields obtained in the absence of added CO, and focus upon the data recorded with excess CO present in the following. The OH yields previously obtained were employed within the model to distinguish direct HO_2 formation from indirect production via the OH + CO reaction. Figure 12.5 shows the temporal profile of HO_2 measured by LIF in a propene ozonolysis experiment, along with the HO_2 model results. The first stage of the experiment illustrates the β-hydroxyalkyl peroxy radical HO_2 interference effect noted above – the HO_2 levels are overestimated. Following addition of CO, the observed HO_2 increases slightly (increased through the conversion of OH to HO_2, offset by removal of the interferant RO_2 species) – this part of the experiment represents the base case scenario for retrieval of the HO_2 yield. In the third part of the experiment, water is added to increase the relative humidity to *ca.* 30%, and the observed HO_2 levels (shown corrected for the LIF system calibration humidity

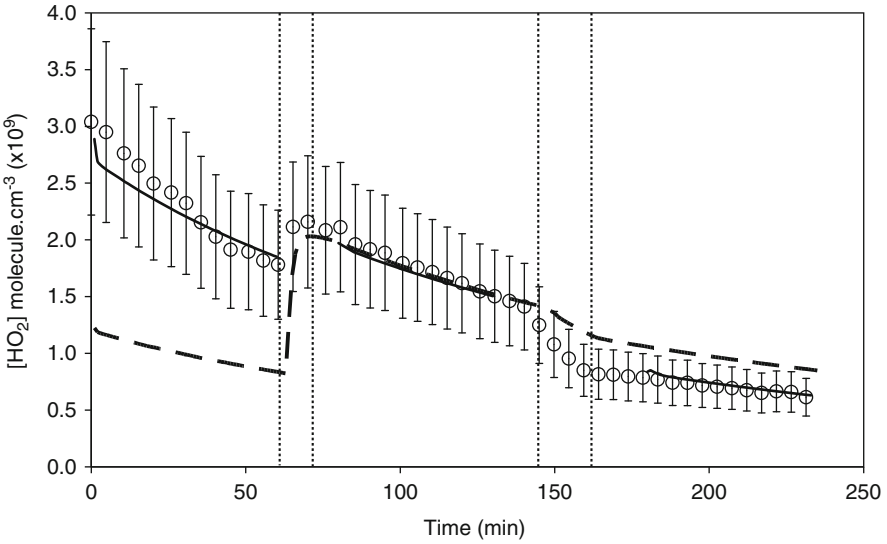

Fig. 12.5 HO_2 production in the ozonolysis of propene (section 1) and its response to the addition of CO (section 2; 62 min +) and H_2O (section 3; 144 min +). Data show the observed concentrations of HO_2 (*open circles*) plus model simulations with direct HO_2 yields of 0.61, 0.09 and 0.02 for sections 1–3 of the experiment respectively (*solid lines*), and for a single fixed yield of 0.09 throughout (*dashed lines*) for a propene ozonolysis

dependence) decrease. The dashed line in Fig. 12.5 represents the modelled HO_2 using an overall yield of 0.09, while the solid lines in sections 1, 2 and 3 show the individually optimized yields of 0.61, 0.09 and 0.02, respectively. The inference from Fig. 12.5 then is that interference effects increase the retrieved "HO_2" in the absence of CO (section 1); the HO_2 yield in the absence of H_2O is 9% (section 2), and upon addition of H_2O, the HO_2 levels decrease, to a greater extent than can be accounted for by the humidity dependence of the HO_2 recombination reaction (which is included in the model), corresponding to a reduction in the HO_2 yield from propene ozonolysis with increasing humidity (section 3).

The dry yields of HO_2 obtained here are compared with those from other studies in Fig. 12.6. The overestimate of the "HO_2 yield" obtained in the absence of CO, from the RO_2 interference, is clearly apparent (filled squares) – these data are not considered further. Our measured yields are in good agreement with measurements for ethene and propene obtained by PERCA, and for isoprene by direct observation by LIF, in the absence of an OH scavenger [22]. The yields obtained in this work are substantially smaller than those reported by Wegener et al. [33] – these values were obtained indirectly from analysis of alkene and ozone turnover in the course of long-duration experiments in the SAPHIR chamber. It is difficult to directly account for the difference between these studies – while the turnover approach is in principle independently sensitive to the HO_x (OH and HO_2) levels present, the sensitivity within the alkene and ozone decays is small (compared with reaction and dilution), reflected in the uncertainty of these values. The HO_2 yields obtained here,

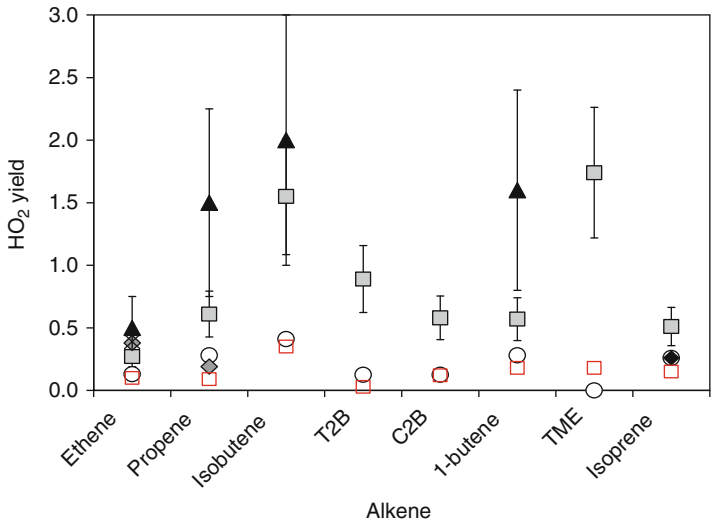

Fig. 12.6 Comparison of HO_2 yields for small chain alkenes investigated during this study with literature values. The abbreviations *T2B*, *C2B* and *TME* are trans-2-butene, cis-2-butene and 2,3-dimethyl-2-butene respectively. *Filled squares* – this work, no CO present (values overestimated due to RO_2 interference). *Open squares* – this work, excess CO experiments (valid HO_2 data); *filled triangles* – Wegener et al. [33]; *light filled diamonds* (ethene, propene) – Qi et al. [27, 28]; *dark filled diamond* (isoprene) – Malkin et al. [22]; *star* (ethene) – Mihelcic et al. [24] and *open circles* – model yields, MCMv3.1

and by Qi et al. [28] and Malkin et al. [22], are in good agreement with those implemented within the MCMv3.1, at least under dry conditions.

The humidity dependence of OH production was not studied in this work; the majority of previous studies have found no evidence for any variation with water vapour (*e.g.* [17] and references therein), although some indications of variations with H_2O have been reported (*e.g.* [33]). As noted above, HO_2 yields decreased upon addition of water vapour for the propene – ozone system (0.09 ± 0.02 to 0.02 ± 0.01). Reductions in HO_2 yields upon addition of water were also observed for ethene (0.10 ± 0.03 to 0.05 ± 0.01 – [1]) and *cis*-2-butene (albeit from a low starting point: 0.03 ± 0.01 to 0.00 ± 0.01), but interestingly not to any significant extent for 2-methyl propene (0.36 ± 0.10 to 0.38 ± 0.10). These data suggest that water vapour is able to intercept (at least part of) the HO_2 formation chemistry in (at least some) alkene ozonolysis reactions. The trend is consistent with the reduction in HO_2 yields observed with increasing humidity by Wegener et al. [33] – where yield reductions of *ca.* 20% were observed for ethene, propene and isobutene (but not for 1-butene) when going from dry conditions to ca. 10 mbar H_2O, albeit with considerable (≈50%) uncertainty. Recently, Leather et al. [20] have reported an increase in the yield of formic acid formation from ethene ozonolysis with increasing humidity, attributed to H_2O reacting with the (stabilized) Criegee intermediate in this system. Together, these studies indicate that the yield of HO_2 from alkene ozonolysis may vary with humidity, implying that competition may occur within the mechanism between radical production through decomposition, and

bimolecular reaction, of the stabilized Criegee intermediate (most likely, through decomposition of the "hot" acid intermediate which results from isomerisation of the *anti*-CI and/or CH_2OO).

12.5 Atmospheric Implications

A constrained zero-dimensional box model was used to quantify the role of alkene ozonolysis to radical production, under ambient conditions observed during the TORCH (Tropospheric Organic Chemistry) field experiment performed in a suburban location to the North-East of London during July and August 2003. This period coincided with an air pollution event and heatwave, leading to elevated ozone and VOC levels compared with the mean for the location and season [21]. The model was constrained to observed levels of long-lived species (NO_x, O_3, H_2O, VOCs, HCHO), meteorological parameters and photolysis rates, and used to calculate the relative contribution of the different (primary) OH and HO_2 production channels, employing the HO_x yields derived from the experiments described above. For OH, ozonolysis was found to account for 29% of primary production (dominated by $O_3 + h\nu/O(^1D) + H_2O$), while for HO_2 ozonolysis accounted for 8% of primary production, which was dominated by aldehyde, particularly HCHO, photolysis (this simple calculation neglects the nested contribution of ozonolysis to the aldehyde loading). Three caveats apply to these values – *total* OH production was dominated by radical cycling, with the reactions of HO_2 with NO and O_3 accounting for 88% of the total flux into OH; HONO photolysis was not included, as HONO observations were unavailable, and is likely to make a substantial contribution, and the ozonolysis radical yields used from this work were those obtained under dry conditions. If, as hypothesised above, radical yields are reduced in the presence of water vapour, and hence potentially other reaction partners (*e.g.* NO), these figures for the importance of ozonolysis in the atmosphere may be regarded as upper limits.

12.6 Conclusions

The production of OH and HO_2 radicals from the ozonolysis of a range of small alkenes has been studied through a simulation chamber approach using the EUPHORE facility, including direct observations of OH and HO_2 via laser-induced fluorescence, with the data obtained analysed in conjunction with a detailed chemical box model to obtain radical yields. OH yields are in agreement with previous measurements, and are consistent with the dominant mechanistic source being the rapid isomerisation and decomposition of *syn*-CIs (Criegee Intermediates) via the hydroperoxide mechanism. Yields of HO_2 were lower than those inferred in some other recent studies, but were in good agreement with those implemented in the Master Chemical Mechanism (version 3.1) under dry conditions. Analysis of atmospheric field data confirmed ozonolysis as a significant source of OH and HO_2 radicals in

the summertime semi-polluted continental boundary layer. Evidence for a reduction in HO_2 yield with increasing humidity was observed for ethene, propene and *cis*-2-butene, implying that these and other similar calculations may overestimate HO_x production from alkene ozonolysis under ambient humidity conditions.

Acknowledgements The contributions of the staff at EUPHORE is gratefully acknowledged, in particular Paco Alacreu, Mónica Vázquez, Mila Rodenas, Amalia Muñoz, and Teresa Vera Espallardo. This work was funded by the UK Natural Environment Research Council (NERC) as part of the TRAPOZ – Total Radical Production from Alkene Ozonolysis project, Grant Ref. NE/E016081/1.

References

1. Alam MS, Camredon M, Rickard AR, Carr T, Wyche KP, Hornsby KE, Monks PS, Bloss WJ (2011) Total radical yields from tropospheric ethene ozonolysis. Phys Chem Chem Phys 13:11002–11015
2. Atkinson R (1997) Gas-phase tropospheric chemistry of volatile organic compounds: 1. alkanes and alkenes. J Phys Chem Ref Data 26:215–290
3. Becker KH (1996) EUPHORE: final report to the European Commission. contract EV5V-CT92-0059. Bergische Universität Wuppertal, Germany
4. Bloss WJ, Lee JD, Bloss C, Heard DE, Pilling MJ, Wirtz K, Martin-Reviejo M, Siese M (2004) Evaluation of the Calibration of a laser-induced fluorescence instrument for the measurement of OH radials in the atmosphere. Atmos Chem Phys 4:571–583
5. Bloss C, Wagner V, Jenkin ME, Volkamer R, Bloss WJ, Lee JD, Heard DE, Wirtz K, Martin-Reviejo M, Rea G, Wenger JC, Pilling MJ (2005) Development of a detailed chemical mechanism (MCMv3. 1) for the atmospheric oxidation of aromatic hydrocarbons. Atmos Chem Phys 5:641–664
6. Calvert JG, Atkinson R, Kerr JA, Madronich S, Moortgat GK, Wallington TJ, Yarwood G (2000) The mechanism of atmospheric oxidation of the alkenes. Oxford University Press, New York
7. Criegee R (1975) Mechanism of ozonolysis. Angew Chem 14:745–752
8. Dillon TJ, Crowley JN (2008) Direct detection of OH formation in the reactions of HO_2 with $CH_3C(O)O_2$ and other substituted peroxy radicals. Atmos Chem Phys 8:4877–4889
9. Donahue NM, Drozd GT, Epstein SA, Presto AA, Kroll JH (2011) Adventures in ozoneland: down the rabbit-hole. Phys Chem Chem Phys 13:10848–10857
10. Fenske JD, Hasson AS, Ho AW, Paulson SE (2000) Measurement of absolute unimolecular and bimolecular rate constants for CH_3CHOO generated by the *trans*-2-butene reaction with ozone in the gas phase. J Phys Chem A 104:9921–9932
11. Fuchs H, Bohn B, Hofzumahaus A, Holland F, Lu KD, Nehr S, Rohrer F, Wahner A (2011) Detection of HO_2 by laser-induced fluorescence: calibration and interferences from RO_2 radicals. Atmos Meas Tech 4:1209–1225
12. Green TJ, Reeves CE, Fleming ZL, Brough N, Rickard AR, Bandy BJ, Monks PS, Penkett SA (2006) An improved dual channel PERCA instrument for atmospheric measurements of peroxy radicals. J Environ Monit 8:530–536
13. Hatakeyama S, Akimoto H (1994) Reactions of Criegee intermediates in the gas phase. Res Chem Intermed 20:503–524
14. IUPAC (2009) International union of pure and applied chemistry subcommittee on gas kinetic data evaluation. http://www.iupac-kinetic.ch.cam.ac.uk/
15. Jenkin ME, Saunders SM, Pilling MJ (1997) The tropospheric degradation of volatile organic compounds: a protocol for mechanism development. Atmos Environ 31:81–104

16. Jenkin ME, Hurley MD, Wallington TJ (2007) Investigation of the radical product channel of the $CH_3C(O)O_2$ + HO_2 reaction in the gas phase. Phys Chem Chem Phys 9:3149–3162
17. Johnson D, Marston G (2008) The gas-phase ozonolysis of unsaturated volatile organic compounds in the troposphere. Chem Soc Rev 37:699–716
18. Johnson D, Lewin AG, Marston G (2001) The effect of Criegee-intermediate scavengers on the OH yield from the reaction of ozone with 2-methylbut-2-ene. J Phys Chem A 105:2933–2935
19. Kuwata KT, Hasson AS, Dickinson RV, Petersen EB, Valin LC (2005) Quantum chemical and master equation simulations of the oxidation and isomerization of vinoxy radicals. J Phys Chem A 109:2514–2524
20. Leather KE, McGillen MR, Cooke MC, Utembe SR, Archibald AT, Jenkin ME, Derwent RG, Shallcross DE, Percival CJ (2011) Acid-yield measurements of the gas-phase ozonolysis of ethene as a function of humidity using Chemical Ionisation Mass Spectrometry (CIMS). Atmos Chem Phys Discuss 11:25173–25204
21. Lee JD, Lewis AC, Monks PS, Jacob M, Hamilton JF, Hopkins JR, Watson NM, Saxton JE, Ennis C, Carpenter LJ, Carslaw N, Fleming Z, Bandy BJ, Oram DE, Penkett SA, Slemr J, Norton E, Rickard AR, Whalley LK, Heard DE, Bloss WJ, Gravestock T, Smith SC, Stanton J, Pillin MJ, Jenkin ME (2006) Ozone photochemistry and elevated isoprene during the UK heatwave of August 2003. Atmos Environ 40:7598–7613
22. Malkin TL, Goddard A, Heard DE, Seakins PW (2010) Measurements of OH and HO_2 yields from the gas phase ozonolysis of isoprene. Atmos Chem Phys 10:1441–1459
23. McGill CD, Rickard AR, Johnson D, Marston G (1999) Product yields in the reactions of ozone with Z-but-2-ene, E-but-2-ene and 2-methylbut-2-ene. Chemosphere 38:1205–1212
24. Mihelcic D, Heitlinger M, Kley D, Musgen P, Volz-Thomas A (1999) Formation of hydroxyl and hydroperoxy radicals in the gas-phase ozonolysis of ethene. Chem Phys Lett 301:559–564
25. Niki H, Maker PD, Savage CM, Breitenbach LP, Hurley MD (1987) FTIR spectroscopic study of the mechanism for the gas-phase reaction between ozone and tetramethylethylene. J Phys Chem 91:941–946
26. Olzmann M, Kraka E, Cremer D, Gutbrod R, Andersson S (1997) Energetics, kinetics, and product distributions of the reactions of ozone with ethene and 2, 3-dimethyl-2-butene. J Phys Chem A 101:9421–9429
27. Qi B, Sato K, Imarnura T, Takami A, Hatakeyama S, Ma Y (2006) Production of the radicals in the ozonolysis of ethene: a chamber study by FT-IR and PERCA. Chem Phys Lett 427:461–465
28. Qi B, Yang B, Wang ZQ, Yang HY, Liu L (2009) Production of radicals in the ozonolysis of propene in air. Sci China B Chem 52:356–361
29. Rathman WCD, Claxton TA, Rickard AR, Marston G (1999) A theoretical investigation of OH formation in the gas-phase ozonolysis of E-but-2-ene and Z-but-2-ene. Phys Chem Chem Phys 1:3981–3985
30. Rickard AR, Johnson D, McGill CD, Marston G (1999) OH yields in the gas-phase reactions of ozone with alkenes. J Phys Chem A 103:7656–7664
31. Saunders SM, Jenkin ME, Derwent RG, Pilling MJ (2003) Protocol for the development of the Master Chemical Mechanism, MCM v3 (Part A): tropospheric degradation of non-aromatic volatile organic compounds. Atmos Chem Phys 3:161–180
32. Siese M, Becker KH, Brockmann KJ, Geiger H, Hofzumahaus A, Holland F, Mihelcic D, Wirtz K (2001) Direct measurement of OH radicals from ozonolysis of selected alkenes: a EUPHORE simulation chamber study. Environ Sci Technol 35:4660–4667
33. Wegener R, Brauers T, Koppmann R, Bares SR, Rohrer F, Tillmann R, Wahner A, Hansel A, Wisthaler A (2007) Simulation chamber investigation of the reactions of ozone with short-chained alkenes. J Geophys Atmos 112. doi:10.1029/2006JD007531
34. Wyche KP, Blake RS, Ellis AM, Monks PS, Brauers T, Koppmann R, Apel EC (2007) Technical note: performance of chemical ionization reaction time-of-flight mass spectrometry (CIR-TOF-MS) for the measurement of atmospherically significant oxygenated volatile organic compounds. Atmos Chem Phys 7:609–620
35. Zador J, Turanyi T, Wirtz K, Pilling MJ (2006) Measurement and investigation of chamber radical sources in the European Photoreactor (EUPHORE). J Atmos Chem 55:147–166